# Melting process and interface instability of highly magnetized solid 3He: Role of the magnetization gradient

Akimoto, H.; Rooijen, R. van; Jochemsen, R.; Frossati, G.; Saarloos, W. van

# Melting Process and Interface Instability of Highly Magnetized Solid $^3$He: Role of the Magnetization Gradient

H. Akimoto,[1,*] R. van Rooijen,[1] R. Jochemsen,[1] G. Frossati,[1] and W. van Saarloos[2]

[1]*Kamerlingh Onnes Laboratorium, Universiteit Leiden, P.O. Box 9504, 2300 RA Leiden, The Netherlands*

[2]*Instituut-Lorentz, Universiteit Leiden, P.O. Box 9506, 2300 RA Leiden, The Netherlands*

(Received 29 February 2000)

We elucidate the melting process of highly magnetized solid $^3$He by observing the magnetization profile and the liquid-solid interface simultaneously. Clear enhancements of magnetization and magnetization gradients at the interface of both the solid and the liquid were observed during melting. These measurements provide a mesoscopic confirmation of the melting scenario of Castaing and Nozières, and explain the long delay before the instability sets in: The magnetization gradient in the liquid leads to an initial suppression of the melting instability, in accordance with our extension of the stability analysis of Puech *et al.* This resolves the discrepancy between theory and experiment.

PACS numbers: 67.80.Jd, 67.65.+z, 68.45.–v

While $^3$He and $^4$He have for a long time served as some of the cleanest model systems to study many of the fundamental collective quantum effects of nature, their remarkable properties have also increasingly been used in the last decade to probe other basic phenomena which are not of a quantum nature by themselves. Examples of helium used as a probe in condensed matter physics and materials science are investigations of the roughening transition, crystallization waves, the Grinfeld instability [1], and phase transitions in disordered media [2,3]. The remarkable melting process of $^3$He that we address here is another "classical" phenomenon made possible by the extraordinary quantum properties of $^3$He and which bears on the fundamentals of interfacial pattern formation.

The growth and melting of solid is accompanied by flows of mass and heat due to the density and entropy differences between the liquid and solid phases. If the two phases have different magnetization in equilibrium, this is accompanied by a magnetization flow. Since $^3$He solid has a much larger magnetization than the liquid, the melting properties are peculiar, and $^3$He is unique in the sense that it allows one to probe the magnetization transfer at the interface and the magnetization flows in the bulk phases.

Castaing and Nozières [4] considered melting of magnetized solid $^3$He on a time scale shorter than the spin-lattice relaxation time. According to their melting scenario, a magnetization boundary layer builds up on the solid side of the interface during melting of magnetized $^3$He. This boundary layer is simply due to the fact that, during the melting, the magnetization in the newly produced liquid is enhanced, and that this in turn enhances the magnetization in the solid near the interface. Bonfait *et al.* [5] suggested that, in analogy to the Mullins-Sekerka–type instability [6] in solidification, the buildup of this boundary layer would render the interface unstable. This suggestion was backed up by a calculation of Puech *et al.* [7]. The situation they analyzed, sketched in Fig. 1(a), is the one often used in theoretical considerations [8], namely, that of a planar interface propagating with constant speed in the absence of magnetization gradients in the liquid. The analysis of Puech *et al.* [7] for this case showed that the interface would be unstable with a typical growth time for the most unstable modes of the order of 0.1 s.

While in earlier experiments [5,9] the melting process could be inferred only from temperature, pressure, and

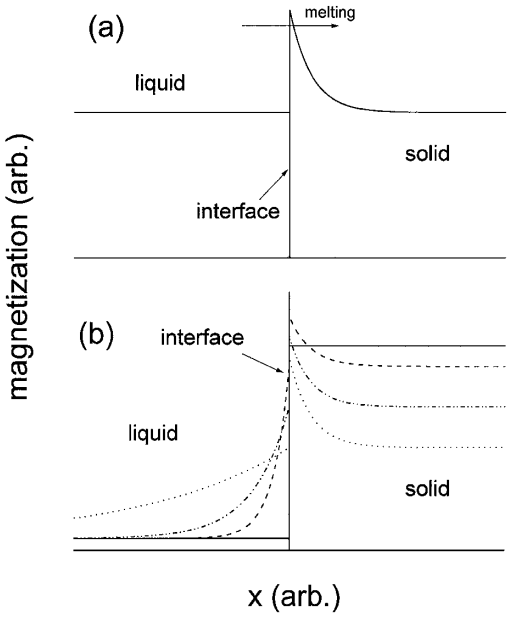


FIG. 1. (a) Sketch of the magnetization profile of a planar interface melting with a constant speed, for which Puech *et al.* [7] performed the linear stability analysis. The magnetization profile falls off exponentially in the solid, while there is no gradient in the liquid. (b) Sketch of the buildup of the magnetization profiles: at the moment the melting starts at $t = 0$ (solid line), and at three successive times during the initial melting phase. Note that, while the boundary layer in the solid is building up, a stabilizing gradient is also building up in the liquid. In the bulk of the solid, to the right, the magnetization relaxes downwards due to the increase in the temperature. Both pictures are drawn in a frame moving with the interface.

 0031-9007/00/85(9)/1894(4)$15.00 

total magnetization measurements, we have also recently been able to follow the melting process visually [10,11]. Our first experiments confirmed the existence of an instability that gave rise to cellular type dendrites, in qualitative agreement with the predictions of Puech *et al.* [7]. However, contrary to naive expectations based on these predictions, the interfacial instability occurred only 10–100 s after the melting started. This delay time depended on the magnetization and experimental protocol. At first sight, this observation appears to be at odds with the finding of Puech and co-workers that the instability should occur within a fraction of a second.

In this Letter, we elucidate the melting process and resolve this apparent contradiction. By using field gradient NMR, we are able to supplement the visual images with measurements of the magnetization profile perpendicular to the interface during the initial transients. The measurements reveal the buildup of a magnetization gradient on both the liquid and the solid side of the interface during the first phase of the melting process. This situation, which is in full accord with what is expected on the basis of simple arguments, is sketched in Fig. 1(b). As our extension of the stability calculation of Puech *et al.* [7] shows, this gradient in the liquid has a strong effect on the melting interface: its sign is such that it stabilizes the interface during the initial phase of the melting and this stabilizing effect overwhelms the destabilizing gradient on the solid side. In agreement with our theoretical results, the interface is found to be unstable only once the magnetization gradient on the liquid side is negligible. At that moment, the situation resembles the one analyzed by Puech *et al.,* as sketched in Fig. 1(a). Indeed, once the instability occurs, it develops in a short time scale.

The experimental apparatus was very similar to the one reported earlier [11,12]. The main difference is that the distance between the windows of the new optical cell, which again has a cylinder shape with a diameter of 5 mm, is only 3 mm. This short distance between the two windows and the nucleation heater at the bottom allows us to establish a proper vertical temperature gradient during the growth of the solid and to obtain a horizontal solid-liquid interface. A magnetic field of 8.9 T is applied vertically. In addition, a vertical field gradient coil was installed so as to measure the magnetization profile *perpendicular to the interface*. The gradient, 0.3 T/m, is applied downwards in order to suppress the spin waves at the interface side. An NMR pickup coil is wound around the optical cell and is tuned at 287 MHz. The magnetization profile of the sample was measured by cw NMR absorption with the frequency sweep method. The time traces of the $^3$He pressure and the magnetization profile were monitored, in addition to the images, at roughly 5 s intervals. The solid was grown by slowly compressing the $^3$He in the chamber. After the growth was finished, the solid was left for 6 to 16 h to cool and to get to equilibrium.

In Fig. 2, a series of the rapid melting images are shown. The first image in Fig. 2 is taken before melting. The bottom of the black line is identified with the interface between solid and liquid. The interface was almost horizontal with a small curvature. After melting starts, the interface stays mostly horizontal and smooth for about 40 s, while the melting velocity is about 15 $\mu$m/s. Then the instability becomes evident, and from this run and a large series of earlier experiments [11] we conclude that the instability typically occurs suddenly.

In Fig. 3, the magnetization profiles are shown during the rapid melting. Note that since we determine the total magnetization in each horizontal slice, and since our optical cell has a circular shape, the magnetization profile of the equilibrium liquid appears curved and semicircular. The large absorption on the high frequency side at $t = 0$ corresponds to the solid. The width of the interfacial region is about 4 kHz in frequency, which corresponds to 0.4 mm, and is due to the fact that the interface is not completely flat and not completely perpendicular to the field gradient. The arrows in Fig. 3 indicate the positions of the interface derived from the images in Fig. 2. Although the position of the arrow at $t = 0$ has some uncertainty and we took the position of the interface at the shoulder of the magnetization step, the displacements between the arrows are precise. During the melting, the magnetization of the bulk part of the solid decreases homogeneously and rapidly due to the heating produced by the melting. The decay of the magnetization in the solid corresponds to the bulk decay rate [13].

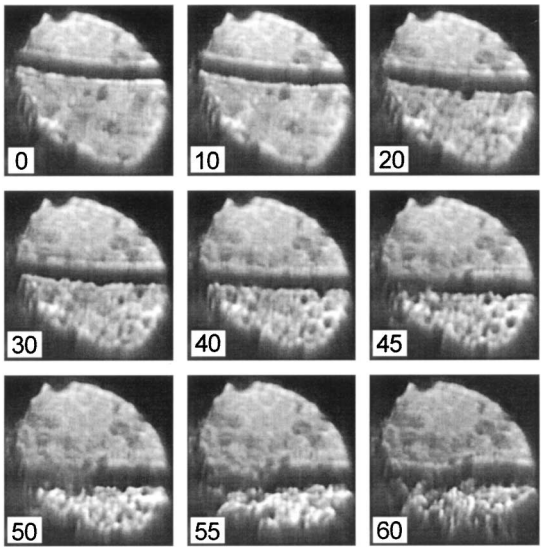


FIG. 2. The images during rapid melting in a 8.9 T magnetic field. The diameter of the images is 4 mm. The number of pixels in the images is 240 × 240 and the pixel size is roughly 13 $\mu$m. The numbers in the images indicate the time in seconds after the beginning of the melting. The aperture time for each image was 1.2 s. The magnetic field is applied vertically. The sample cell has 3 mm depth along the path of the light.

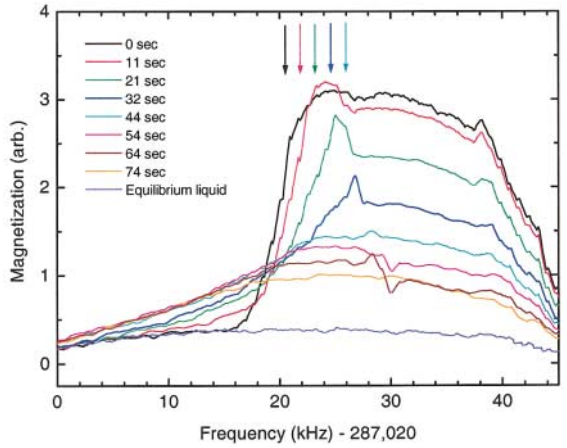


FIG. 3 (color). The magnetization profiles during the rapid melting for each 10 s. The vertical field gradient is about 0.3 T/m, which corresponds with 10 kHz/mm. The magnetic field is 8.9 T, and the initial temperature is 5 mK. The arrows indicate the positions of the interface.

The measurements in Fig. 3 are the first mesoscopic confirmation of the melting scenario of Castaing and Nozières [4]: when the magnetized solid melts, it produces liquid with enhanced magnetization, and a magnetization boundary layer in the solid is built up. As we anticipated in Fig. 1(b), our measurements show that this initially leads to the buildup of a magnetization gradient in the liquid, whose sign is opposite to the one on the solid side of the interface, and hence, as we shall show, stabilizes the interface. Moreover, from our visual images, we find that the instability happens at $t \approx 40$ s when the magnetization of the bulk solid is almost the same as that of the liquid, and that at that time the magnetization gradient in the liquid near the interface is almost zero.

Our assertion that the magnetization gradient in the liquid stabilizes the interface during the initial transient phase is fully supported by our extension of the linear stability calculation of Puech *et al.* [7]. For the unperturbed planar interface, we take the solid at $x > 0$ in a frame moving with the instantaneous planar interface velocity $V$. The magnetization profiles in the direction perpendicular to the interface are denoted by $M_l(x)$ and $M_s(x)$ for the liquid and the solid, respectively. Upon writing the perturbation $\xi$ of the interface position as

$$\xi(k,t) = \xi_k \exp(iky + \gamma t), \tag{1}$$

we find, after linearizing the magnetization transport equations in $\xi$, the following relation between $\gamma$ and $k$:

$$\gamma = -\frac{(\partial M_s/\partial x)^{\text{int}}}{\Delta M}(D_s q_s - V) - \frac{D_l q_l (\partial M_l/\partial x)^{\text{int}}}{\Delta M} - \frac{\tilde{\alpha}\phi k^2}{(\Delta M)^2}[D_s q_s \chi_s + D_l q_l \chi_l + V(\chi_l - \chi_s)]. \tag{2}$$

Here $\Delta M = M_s^{\text{int}} - M_l^{\text{int}}$ and the superscript "int" denotes the value of the planar magnetization profiles at the interface position. All other notations are those of Ref. [7]; e.g., $D_s$, $D_l$, $\chi_s$, and $\chi_l$ are the spin diffusion coefficient and susceptibility of the liquid and the solid, and $\tilde{\alpha}$ is the solid-liquid surface stiffness. Furthermore, since the spatial decay rates $q_l$ and $q_s$ of the perturbed magnetization into the liquid and solid are functions of $\gamma$ and $k$ through [7],

$$D_s(q_s^2 - k^2) - Vq_s = \gamma,$$
$$D_l(q_l^2 - k^2) + Vq_l = \gamma. \tag{3}$$

Equation (2) implicitly determines the dispersion relation of the temporal growth factor $\gamma(k)$.

Since $(\partial M_s/\partial x)^{\text{int}}$ in Eq. (2) is negative and $D_s q_s - V > 0$, except for exceedingly high interface velocities, the first term tends to make $\gamma$ positive. Consequently, it is the destabilizing term due to the gradient in the solid. The last term, due to the surface stiffness, is always stabilizing. When the liquid gradient $(\partial M_l/\partial x)^{\text{int}} = 0$, Eq. (2) reduces to the result derived in Ref. [7], and the remaining terms then lead to a Mullins-Sekerka–type instability. However, Eq. (2) shows that a positive liquid gradient leads to stabilization. Moreover, since the liquid spin diffusion coefficient, $D_l$, is typically much larger than $D_s$ (their ratio is strongly temperature and pressure dependent), we see that the instability can occur only when the liquid gradient is very small—otherwise, the sum of the first two terms is negative and there is no instability. Thus, this linear stability calculation fully confirms our experimental observation that *the interface remains stable as long as there is a positive magnetization gradient on the liquid side.* Moreover, although the precise values for the length scale and growth time of the most unstable mode depend quite sensitively on the parameter values used, once the interface is unstable, the time scale on which the instability occurs is predicted to be small (an order of a fraction of a second). This is reasonably consistent with our experimental observations that the instability develops in two successive frames.

We finally note the following points concerning the data: (i) Although we clearly observe the interface instability, in agreement with the theoretical predictions, our observations do not rule out that under some circumstances nucleation of the liquid phase occurs in the bulk of the solid as well. There are actually some hints that this happens in the images of Fig. 2; we have not studied the dependence of this effect on depressurization rate, temperature, etc., systematically.

(ii) In the initial phase of the melting, the interface dynamics is actually diffusion limited, i.e., limited by the buildup of the enhanced magnetization boundary layer in the solid. From the steep drop of the magnetization on the solid side (the right side in Fig. 3) of the boundary layer, we estimate an upper bound for the width of this layer of

about 0.1 mm, which is consistent with a spin diffusion coefficient of the order of $10^{-5}$ cm$^2$/s. Our scenario implies that the point when the liquid gradient becomes negligible, $(\partial M_l/\partial x)^{\text{int}} \approx 0$, is close to the point where a crossover from diffusion limited growth to interface kinetics dominated growth occurs [14].

(iii) The data in Fig. 3 show a wiggle in the magnetization profiles after the instability has occurred. This is an indication that the driving force for the solid magnetization to relax down is large (possibly due to the relatively high temperature at late times), and that therefore minority spins, whose magnetization is opposite to the magnetic field, diffuse back from the liquid into the solid. This causes the liquid magnetization to go up, and the solid magnetization near the outer edge to go down. The development of the wiggly feature in the data in a few seconds is again consistent with a spin diffusion coefficient of the order of $10^{-5}$ cm$^2$/s.

In conclusion, by combining visual images of the melt process with measurements of the magnetization profiles, we have confirmed the Castaing-Nozières melting scenario of magnetized $^3$He. Moreover, when the existence of magnetization gradients in the liquid is taken into account in the stability calculation of the interface, the observations are fully consistent with the existence of the interface instability predicted by Puech *et al.*—the suppression of the instability in the early phase of the melting is due to the existence of a magnetization gradient in the liquid.

We thank A. Marchenkov for his contribution in earlier stages of this work. W. vS. also thanks P. Nozières and C. Caroli for stimulating discussions. This work was partly supported by the Stichting Fundamenteel Onderzoek van de Materie (FOM), which is financially supported by the Nederlandse Organisatie voor Wetenschappelijk Onderzoek (NWO).

*Email address: hikota@physics.umass.edu
Present address: Hasbrouck Laboratory, Department of Physics, University of Massachusetts, Amherst, MA 01003.

[1] S. Balibar and P. Nozières, Solid State Commun. **92**, 19 (1994).
[2] See, e.g., N. Mulders and M. H. W. Chan, Phys. Rev. Lett. **75**, 3705 (1995).
[3] K. Matsumoto, J. V. Porto, L. Pollack, E. N. Smith, T. L. Ho, and J. M. Parpia, Phys. Rev. Lett. **79**, 253 (1997).
[4] B. Castaing and P. Nozières, J. Phys. (Paris) **40**, 257 (1979).
[5] G. Bonfait, L. Puech, A. S. Greenberg, G. Eska, B. Castaing, and D. Thoulouze, Phys. Rev. Lett. **53**, 1092 (1984).
[6] W. W. Mullins and R. F. Sekerka, J. Appl. Phys. **35**, 444 (1964).
[7] L. Puech, G. Bonfait, and B. Castaing, J. Phys. (Paris) **47**, 723 (1986).
[8] See, e.g., J. S. Langer, Rev. Mod. Phys. **52**, 1 (1980); K. Kassner, *Pattern Formation in Diffusion-Limited Crystal Growth* (World Scientific, Singapore, 1996).
[9] A review is given in G. Bonfait, L. Puech, and A. Schuhl, in *Helium Three,* edited by W. P. Halperin and L. P. Pitaevskii (Elsevier, New York, 1990).
[10] A. Marchenkov, Ph.D. thesis, Leiden University, 1997.
[11] A. Marchenkov, H. Akimoto, R. van Rooijen, R. Jochemsen, and G. Frossati, Phys. Rev. Lett. **83**, 4598 (1999).
[12] R. Wagner, P. J. Ras, P. Remeijer, S. C. Steel, and G. Frossati, J. Low Temp. Phys. **95**, 715 (1994); H. Akimoto, R. van Rooijen, A. Marchenkov, R. Jochemsen, and G. Frossati, Physica (Amsterdam) **255B**, 19 (1998).
[13] M. Chapellier, M. Bassou, M. Devoret, J. M. Delrieu, and N. S. Sullivan, Phys. Rev. B **30**, 2940 (1984); M. Chapellier, M. Bassou, M. Devoret, J. M. Delrieu, and N. S. Sullivan, J. Low Temp. Phys. **59**, 45 (1985).
[14] Technically, this becomes clear by noting that, in the case sketched in Fig. 1(a), the interface velocity is undetermined if one does not take interface kinetics into account. In the language of temperature diffusion dominated crystal growth, the crossover point corresponds to the case of unit undercooling.